water

MDPI

Article

Green Synthesis and Characterization of LED-Irradiation-Responsive Nano ZnO Catalyst and Photocatalytic Mineralization of Malachite Green Dye

Brijesh Pare [1], Veer Singh Barde [1,*], Vijendra Singh Solanki [2,*], Neha Agarwal [3], Virendra Kumar Yadav [4], M. Mujahid Alam [5], Amel Gacem [6], Taghreed Alsufyani [7], Nidhal Ben Khedher [8,9], Jae-Woo Park [10], Sungmin Park [10] and Byong-Hun Jeon [11,*]

1 Laboratory of Photocatalysis, Department of Chemistry, Govt. Madhav Science PG College, Ujjain 456010, Madhya Pradesh, India
2 Department of Chemistry, School of Liberal Arts and Sciences, Mody University of Science and Technology, Lakshmangarh 332311, Rajasthan, India
3 Department of Chemistry, Navyug Kanya Mahavidhyalay, Lucknow 226004, Uttar Pradesh, India
4 Department of Bioscience, School of Liberal Arts and Sciences, Mody University of Science and Technology, Lakshmangarh 332311, Rajasthan, India
5 Department of Chemistry, Faculty of Science, King Khalid University, Abha 61413, Saudi Arabia
6 Department of Physics, Faculty of Sciences, University 20 Août 1955, Skikda 21000, Algeria
7 Department of Chemistry, College of Science, Taif University, P.O. Box 11099, Taif 21944, Saudi Arabia
8 Department of Mechanical Engineering, College of Engineering, University of Ha'il, Ha'il 81451, Saudi Arabia
9 Laboratory of Thermal and Energy Systems Studies, National School of Engineering of Monastir, University of Monastir, Monastir 5000, Tunisia
10 Department of Civil and Environmental Engineering, Hanyang University, 222-Wangsimni-ro, Seongdong-gu, Seoul 04763, Korea
11 Department of Earth Resources & Environmental Engineering, Hanyang University, 222-Wangsimni-ro, Seongdong-gu, Seoul 04763, Korea
* Correspondence: barde.veeru90@gmail.com (V.S.B.); vijendrasingh0018@gmail.com (V.S.S.); bhjeon@hanyang.ac.kr (B.-H.J.)

Abstract: The green synthesis of nanoparticles is an emerging branch of nanotechnology in recent times, as it has numerous advantages such as sustainability, cost-effectiveness, biocompatibility, and eco-friendliness. In the present research work, the authors synthesized ZnO nanoparticles (ZnO NPs) by a green and eco-friendly method. The synthesized ZnO NPs were characterized by X-ray diffraction (XRD), field emission scanning electron microscopy (FESEM), and Fourier transform infrared (FTIR) spectroscopic techniques. The calculated average crystallite size of ZnO NPs was observed at 36.73 nm and FESEM images clearly showed the cylindrical shape of nanoparticles. The absorption peak at 531 cm^{-1} was observed in the FTIR spectrum of the ZnO NPs sample, which also supports the formation of the ZnO wurtzite structure. Finally, the synthesized ZnO NPs potential was analyzed for the remediation of malachite green from an aqueous solution. The ZnO NPs showed a desirable photocatalytic nature under LEDs irradiation.

Keywords: nanoparticles; zinc oxide; photocatalytic degradation; wastewater; green chemistry

check for updates

Citation: Pare, B.; Barde, V.S.; Solanki, V.S.; Agarwal, N.; Yadav, V.K.; Alam, M.M.; Gacem, A.; Alsufyani, T.; Khedher, N.B.; Park, J.-W.; et al. Green Synthesis and Characterization of LED-Irradiation-Responsive Nano ZnO Catalyst and Photocatalytic Mineralization of Malachite Green Dye. *Water* **2022**, *14*, 3221. https://doi.org/10.3390/w14203221

Academic Editor: Chengyun Zhou

Received: 12 September 2022
Accepted: 11 October 2022
Published: 13 October 2022

Publisher's Note: MDPI stays neutral with regard to jurisdictional claims in published maps and institutional affiliations.

1. Introduction

Heterogeneous photocatalysis is a sustainable and green technology used for contaminated water treatment and recycling [1]. It is considered a suitable technique because of its cost-effectiveness, eco-friendliness, high efficiency, and broad applicability and offers great potential for the overall mineralization of hazardous materials from the environment. Almost complete degradation and mineralization of organic pollutants such as pesticides, herbicides, phenols, antibiotics, hydrocarbons, plastics, etc., are achieved even under mild cases of temperature and pressure [2–5]

Numerous semiconductor materials, such as titanium dioxide (TiO_2), zinc oxide (ZnO), and silica (SiO_2) [6], Cu/Cu@UiO-66 [7], are presented as promising photocatalysts. There are several investigators who worked on TiO_2 and ZnO as photocatalysts owing to their unique and extraordinary photocatalytic properties, such as a non-toxic nature, economically viability, chemical stability, high reactivity, etc., but ZnO has the ability to show photocatalytic efficiency in both the ultraviolet (UV) and visible light. Youji Li et al., improved the photocatalytic efficiency of TiO_2 in visible light by doping N and successfully degraded acid orange 7 dye through visible-light-responsive N-doped mesoporous titania on carbon fibers in 2015 [8]. In the year 2017, Lin Xiao et. al. fabricated a visible-light-driven photocatalyst composed of mesoporous TiO_2 (MT) doped with Ag^+-coated graphene (MT-Ag/GR) and degraded methylene blue dye [9]. Yufen Gu et al., in 2022, synthesized $ZnSn(OH)_6$ (ZSO) by hydrothermal method and degraded methylene blue and Hexadecyl trimethyl ammonium Bromide-ZSO (CTAB-ZSO) [10]. Recently, Liexiao Li et al., fabricated a flower-like $Bi_2O_2CO_3$ photocatalyst and studied its photocatalytic efficiency by the reduction in Cr (VI) in the year 2022 [11].

There is always a need to synthesize a new photocatalyst to fulfil this purpose and try to improve the catalytic efficiency of ZnO by tailoring its particle size, amount of oxygen defects, facets, and surface area modification [12].

In the present scenario, nanosized materials have gained much more focus due to their novel physical properties (such as structural, electronic, and thermal), which are of high scientific interest in basic and applied scientific fields, such as catalysts, sensors, photoelectron devices, and highly effective and working devices [13,14]. In this paper, we synthesized nanostructured ZnO, which has a great advantage in photocatalytic reactions due to its large surface-to-volume ratio and catalytic efficiency [15–18]. The catalytic potential of ZnO NPs was tested by the kinetic study of malachite green (MG) dye under eco-friendly LEDs irradiation. LEDs (p-n junction semiconductor devices) irradiations were chosen as the source of light since they have high and stable energy efficiency, are economically viable, provide continuous exposure of light as compared to traditional energy sources, and are eco-friendly, since conventional light sources are made up of mercury filament, which is hazardous for the environment [19–21].

Recently, ZnONPs were successfully synthesized from the *Manilkara zapota*, *Lipia adoensis*, and *Passiflora caerulea.* In this study, the investigators used the sapota plant since the plant contains different reducing phytoconstituents, such as alkaloids, phenolic compounds, sterols, amino acids, terpenoids, vitamins, etc., which can reduce metallic ions into metal nanoparticles [22–25].

Sapota plant leaf extract was used to synthesize ZnO NPs. The sapota plant belongs to the Sapotaceae family, of the *Pouteria sapota* (*Latin name*) species, and the botanical name is *Manilkara zapota.* The sapota plant is cultivated between 15 °C and 38 °C temperatures in moist tropic or subtropical areas [26].

In this mechanism, the electron of the valence band gets promoted into the conduction band on the irradiation of the light on the nanoparticles in the aqueous medium. The OH^- ions lose their electrons on the valence band and form hydroxyl radicals, which are responsible to oxidize dye molecules. Simultaneously, oxygen reduced by the electrons of the conduction band form $O_2^{\cdot}$ radicals (Figure 1) [27].

Various reaction parameters, such as the effect of change in Fenton's reagent concentration, CO_2, and COD measurements, and the effect of the bubbling of N_2 and O_2 purging, were evaluated during MG dye degradation. All the observed results are correlated and the improved catalytic efficiency is interpreted based on the structural and morphological findings of the prepared nanosized ZnO.

In the present study, authors first synthesized Pouteria-sapota-mediated zinc oxide nanoparticles. Further, the confirmation of the formation of the particle and its purity was analyzed using sophisticated instruments such as FESEM, XRD, and FTIR. The potential of the synthesized ZnO NPs was assessed for the remediation of MG dye under light-emitting diode conditions. The object was to develop a green route for the synthesis of zinc oxide nanoparticles and their potential to eliminate the MG dye from the aqueous solution efficiently.

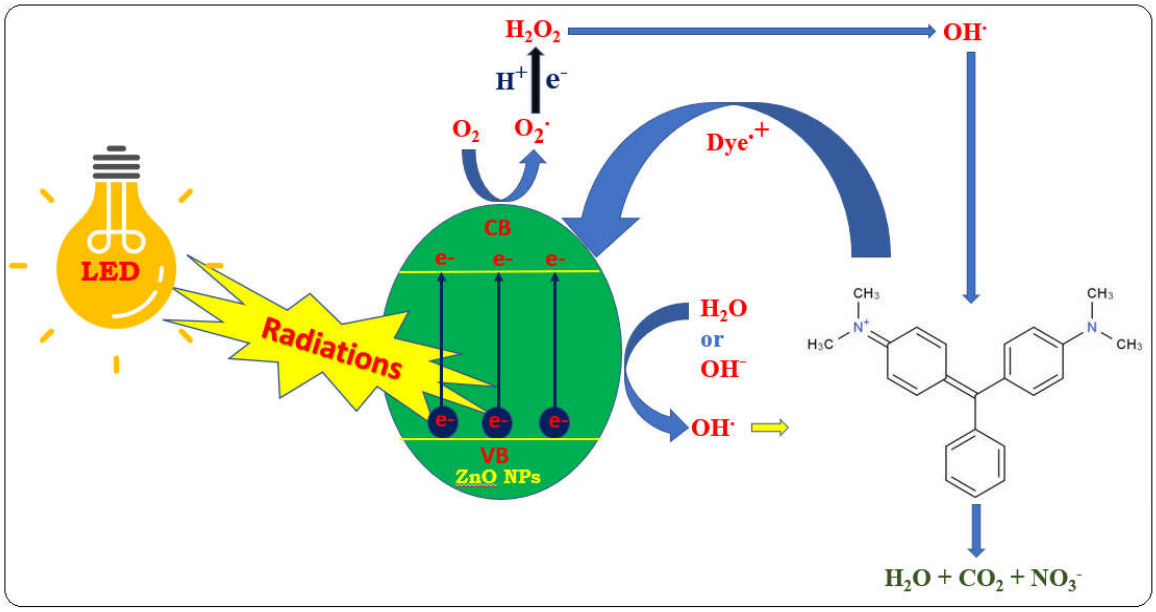

Figure 1. Physical mechanism of degradation of dye by NPs.

2. Experimental Analysis

2.1. Sapota Plant Leaf Extraction

About 100 g of sapota plant (*Manilkara zapota*) leaves was obtained from the university campus of the Lakshmangarh (India) area in the summer season and washed with double-distilled water to remove the dust and dirt present on the leaves. Leaves were air-dried and ground into fine powder in the cleaned mortar with 400 mL of double-distilled water. The liquid was transferred into a 500 mL beaker and concentrated by heating on a hot plate at 60 °C temperature for 1 h with continuous stirring. The suspension was cooled, filtered, and used for the preparation of ZnO NPs [28].

2.2. Synthesis of Nanostructured ZnO

ZnO NPs was prepared by using the leaf extract of the sapota plant. Here, about 100 mL of aqueous solution zinc nitrate (0.45 mol L^{-1}) was prepared in double-distilled water. After that, 30 mL of leaf extract and 50 mL of zinc nitrate solution were mixed drop by drop along with continuous stirring. Then, the beaker was covered by the aluminium sheet for 2 h at 30 °C. The developed particles were carefully washed with double-distilled water and kept in an oven at 60 °C. Finally, the ZnO NPs were calcinated in a muffle furnace at 300 °C for 6 h [29].

2.3. Experimental Procedure

The photocatalytic mineralization of the MG dye solution was conducted in a specially designed double-walled special glass vessel, which maintained constant temperature during the experiment. During a typical photocatalytic experiment, 100 mL of MG dye solution and nanosized ZnO were taken in a slurry-type batch reactor. After stirring for 10 min, the mixture was placed in the dark for 30 min to attain absorption–desorption equilibrium. A slurry containing aqueous dye solution and ZnONPs was then irradiated under the LEDs (250W). After 3 min of time interval, the absorbance of the solution was taken after centrifugation by spectrophotometer. Variation in absorption spectra was measured at 400–620 nm λ_{max} on a spectrophotometer (Systronic Model No.166). A Lux-meter (Lutron LX-101) was used to measure the intensity of visible light. The mineralization efficiency of the process was calculated as:

$$\% \text{ efficiency} = \frac{C_0 - C}{C_0} \times 100$$

where C_0 = initial COD/absorbance of MG dye solution before the experiment, C = final COD/absorbance of MG dye solution after the experiment.

2.4. Characterization of the ZnO Nanoparticle

The X-ray pattern of the prepared ZnO NPs was recorded on the PANalytical Empyrean diffractometer and studied in the range of 20–80° (2θ). The average crystallite size of the nanosized ZnO was determined with the help of the Scherrer formula.

$$D = K\frac{\lambda}{\beta\cos\theta}$$

The surface morphology and mean particle size of the sample were analyzed by a field scanning electron microscope (FESEM). The presence of functional groups in the sample was identified by Fourier transform infrared spectroscopy (FTIR) by using Bruker model ALPHA FTIR.

3. Results and Discussions

3.1. Structural Studies of ZnO Nanoparticle

The intense and narrow peaks from the XRD suggest that the product has good crystalline morphology (Figure 2). The diffraction of the peaks around 31.46°, 34.41°, 36.57°, 47.66°, 56.72°, 62.70°, and 67.95° were indexed to (100), (002), (101), (102), (110), (103), and (112) planes, respectively, which confirmed the synthesis of ZnO NPs as wurtzite-type (hexagonal structure). The d-values and lattice parameters of ZnO NPs were determined [a = b = 3.256 A° and C = 5.220 A° (calculated values) and a = b = 3.250 A° and 5.207 A°] according to JCPDS 36-1451, which are favored to the JCPDS data file for ZnO powder. The calculated average crystallite size of ZnO nanoparticles was observed at 36.73 nm with the help of the Debye–Scherrer formula [30–32]. Similar results were also obtained by Hawwary et al., 2021 and Degefa et al., 2021, where the peaks were also obtained at 31.77, 34.43, 36.36, 47.55, 56.60, and 62.87 [33–35]. The major peak was at 36.6°. The above result shows the crystalline form of the wurtzite type.

The FESEM images (Figure 3) show the general surface morphology of nanosized ZnO. It indicated that the particles are cylindrical in shape and have an average particle size in the range of 20–30 diameter and 150 nm length. Degefa et 2021 also obtained similar type of ZnO NPs by using extracts of onion [34]. Modi et al., 2022 also reported the synthesis of ZnO NPs by using onion peel extracts with similar morphology [32]. Spoiala et al., 2021 also obtained ZnO NPs of similar morphology [36].

Figure 4 shows a typical FTIR spectrum of ZnO NPs. The characteristic band at 531 cm^{-1} and 589 cm^{-1} is assigned to the stretching vibrations of the Zn-O bond. This confirms the formation of ZnO NPs. A few investigators have also obtained bands in the region of 400–500 cm^{-1}, but here we performed analysis from 500 onwards. Spoiala et al., 2021, also obtained bands in the region of 419 to 469 cm^{-1}, which were assigned to the Zn-O bond [36].

A small band at 1510 cm^{-1} could be due to the precursor material used for the synthesis of ZnO NPs, i.e., zinc nitrate. So, the COOH group and OH are present in the region of 1500 to 1650 cm^{-1}. This precursor might have failed to take part in the reaction and could not transform into ZnO NPs [37,38]. The formation of the ZnO wurtzite structure (Figure 4) in the sample was also supported by the XRD and FESEM [39,40].

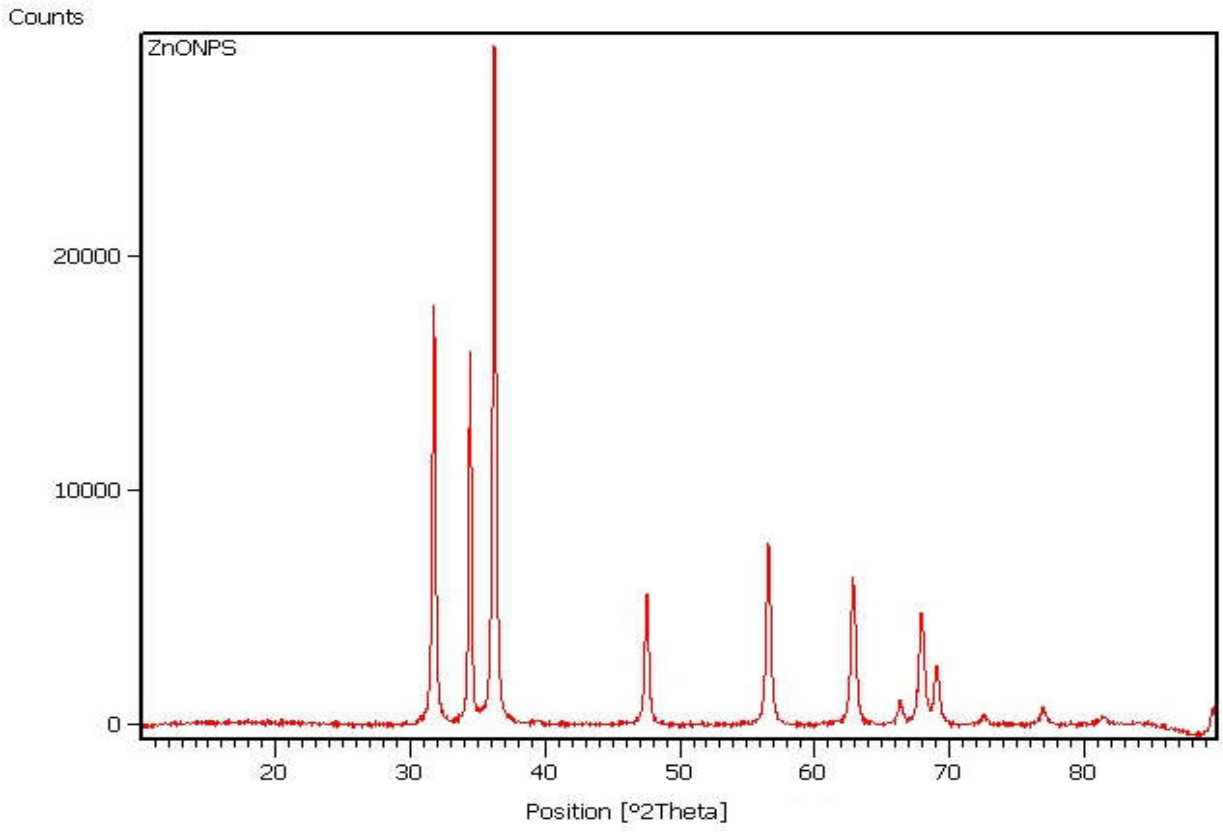

Figure 2. XRD pattern of ZnO NPs.

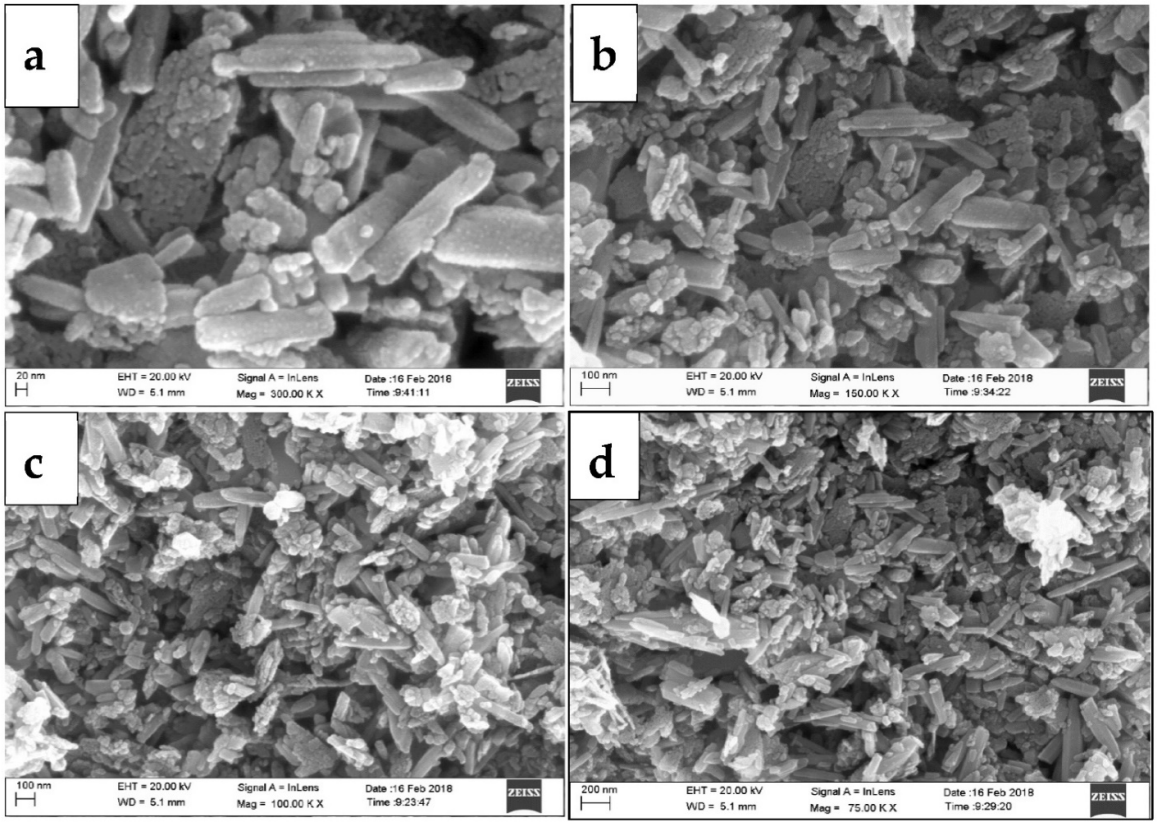

Figure 3. FESEM micrographs of ZnO NPs (**a**–**d**).

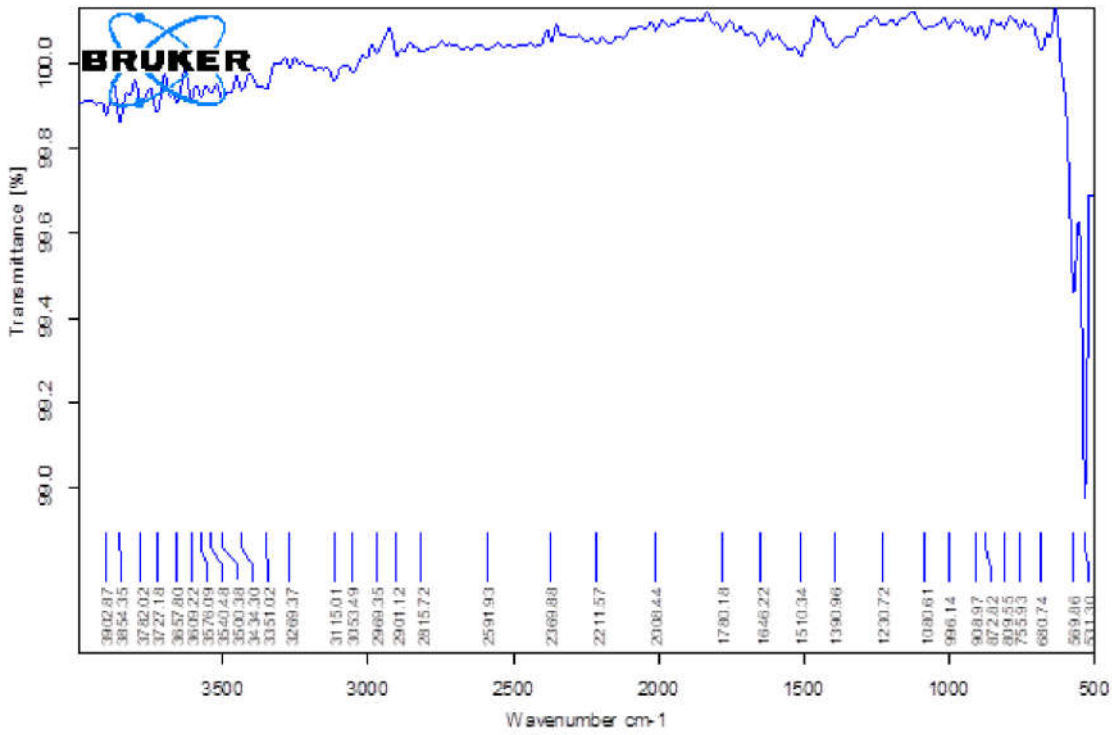

Figure 4. FTIR spectrum of ZnO NPs.

3.2. Photocatalytic Experiments

In this study, the photocatalytic efficiency of the nanosized ZnO NPs was observed by the degradation of MG dye. The degradation rate was very low when only visible light was given to the dye solution. In the absence of ZnO NPs and without LEDs irradiation, no degradation was observed. Both LEDs light and ZnO NPs were essential for the mineralization of the MG dye solution. For the confirmation of the photocatalytic mineralization process, we studied different parameters by optimization of the reaction conditions.

3.2.1. Effect of Change in Fenton's Reagent Concentration

A mixture of ferrous ions and H_2O_2 known as Fenton's reagent was used as a powerful oxidant for organic pollutants. Among advanced oxidation processes, catalytic oxidation using Fenton's reagent and similar reagents is a prominent procedure for effective dye degradation due to its low cost and lack of toxicity. The efficiency of Fe^{3+}/H_2O_2 has been investigated for the mineralization of MG dye by ZnO NPs and visible light. Firstly, we tested the photodegradation of MG dye under different molar ratios. Upon irradiation of the $Fe^{3+}/H_2O_2/ZnO/MG$ method in the presence of LEDs irradiations, we found improved degradation of the MG dye, as compared to the dye solution without ZnO NPs (Figure 5) [41–43].

3.2.2. Measurement of Chemical Oxygen Demand (COD) and CO_2

The COD test has commonly been used to measure the presence of organic waste and permits the measurement of O_2 necessary for the mineralization of the organic dye into CO_2 and H_2O. The COD of the MG-containing solution was determined by pre- and post-treatment of the MG dye solution. The mineralization and decolorization of dye are indicated by a considerable reduction in COD value. The decrease in the COD (chemical oxygen demand) values from 270 mg/L and enhancement in CO_2 values in 115 min in the presence of LEDs irradiation confirmed the complete oxidation as well as mineralization of the treated dye solution [44,45]. The results are shown in Figure 6a,b.

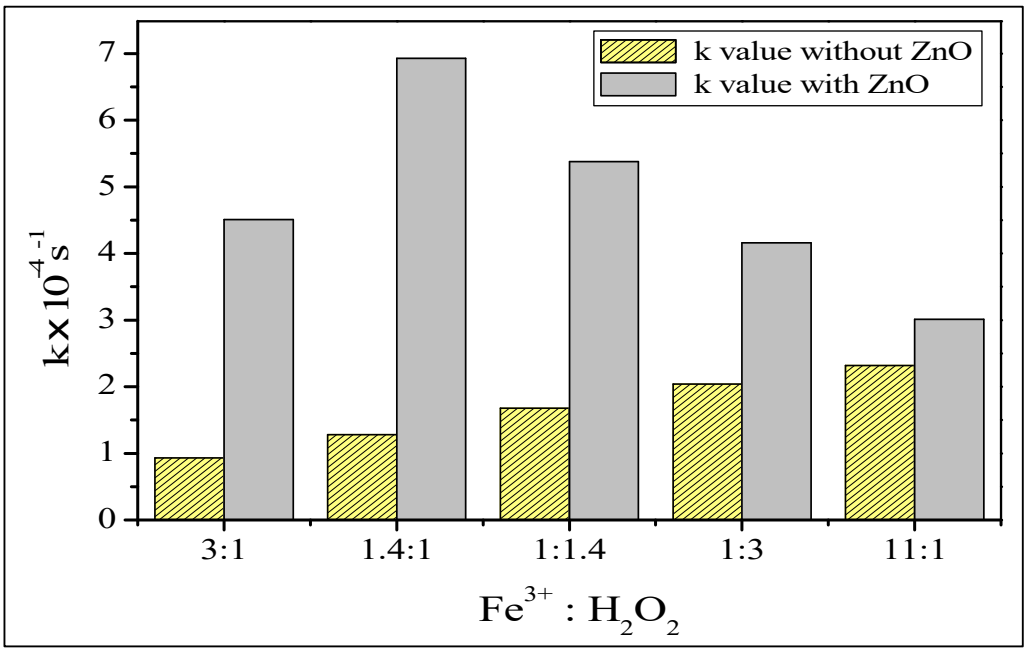

Figure 5. Effect of change in Fenton's reagent concentration.

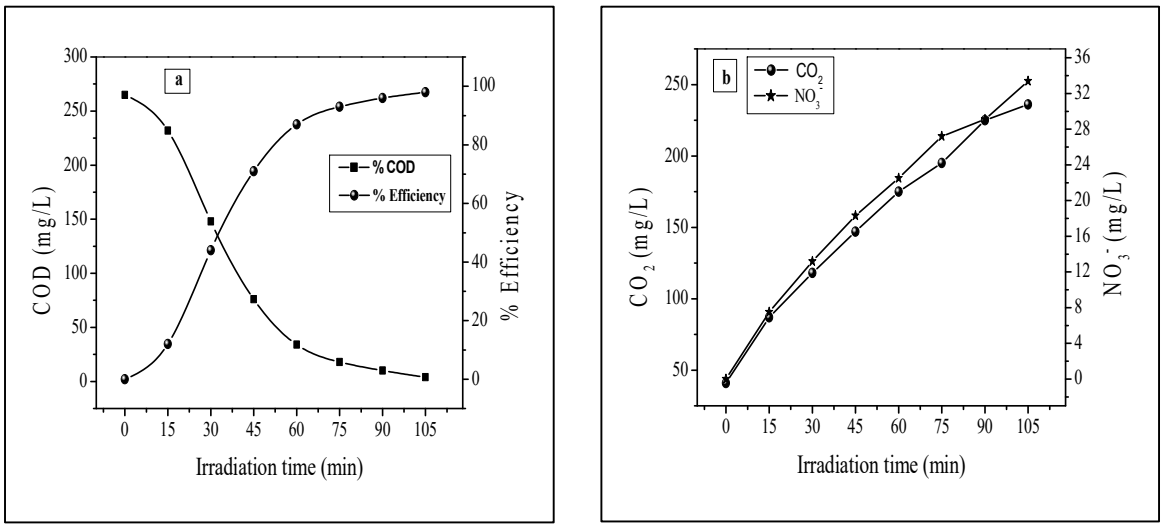

Figure 6. (**a**) measurement of COD removal (**b**) Measurement of CO_2 and nitrate removal.

3.2.3. Effect of Bubbling of N_2 and O_2 Purging

For this test, pure nitrogen and oxygen were purged into the photo-reactor in order to study their effect on the photocatalytic mineralization of MG dye. Oxygen is another important oxidizing agent and not only helps in the degradation of dye but reduces electron-hole recombination as well [46]. The graph showed that the degradation of MG was tremendously retarded by the bubbling of pure N_2 but increased rapidly on bubbling O_2 through the dye solution. The results are shown in Figure 7.

3.2.4. Effect of Other Photocatalysts

Different photocatalysts were tested, and it was found that ZnO NPs are more suitable to degrade MG dye, as compared to other photocatalysts. The rate constant values for the ZnO NPs were 3.4×10^{-4} s^{-1}. The order of efficiency of the tested photocatalysts is: ZnO > TiO_2 > BiOCl > $BaCrO_4$ > CdS, as shown in Table 1.

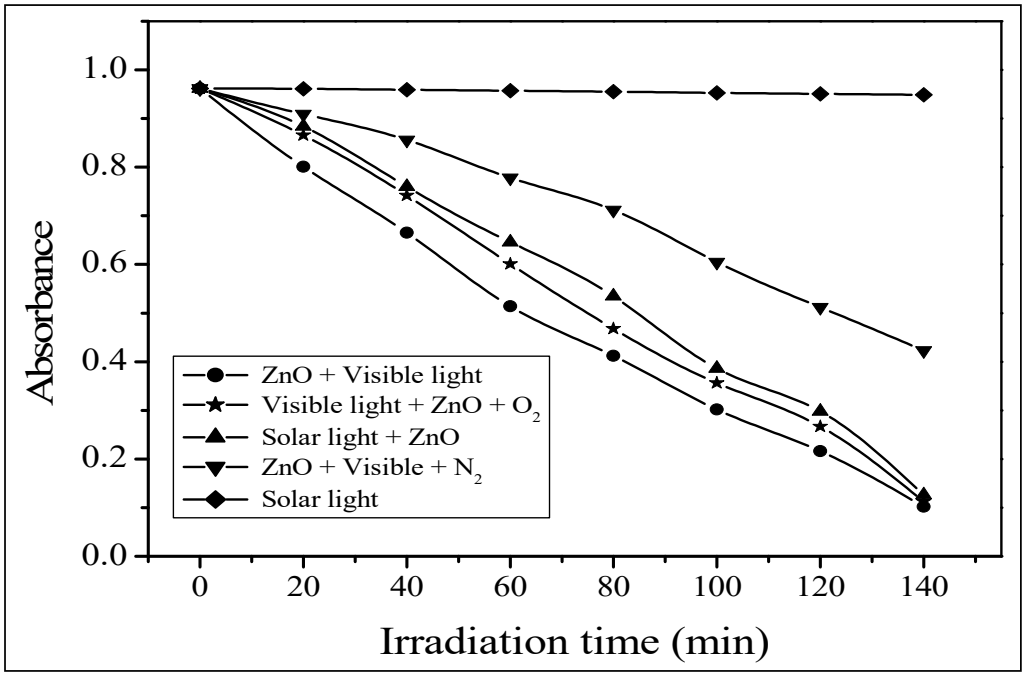

Figure 7. Effect of bubbling of N_2 and O_2 purging.

Table 1. Effects of other photocatalysts.

Photocatalyst	Bandgap (eV)	$k \times 10^{-4}$ s^{-1}
ZnO	3.2	3.4
BiOCl	3.6	3.0
TiO_2	3.1	3.1
$BaCrO_4$	2.6	2.6
CdS	2.1	2.0

3.2.5. Mechanism of Malachite Green Dye Degradation

Previous studies based on the degradation of organic pollutants revealed that hydroxyl radical (OH) is an important oxidizing agent and plays a crucial role in the mineralization of organic pollutants in the aqueous medium. The electron-hole pairs are produced when aqueous ZnO suspension is irradiated. The generated electron-hole pairs can interact with the dye separately. These VB holes oxidize OH^- or H_2O into active $^{\bullet}OH$ radicals, while CB electrons form superoxide radicals ($O_2^{\bullet -}$) by a reduction in O_2 [47,48]. The overall mechanism can be summarized as:

$$ZnO + h\nu_{visible} \rightarrow \text{nanosized ZnO}\left(h^+_{VB} + VB + e^-_{CB}\right) \quad (1)$$

$$ZnO\left(h^+_{VB}\right) + H_2O \rightarrow ZnO + H^+ + OH^{\bullet} \quad (2)$$

$$ZnO\left(h^+_{VB}\right) + OH^- \rightarrow ZnO + OH^{\bullet} \quad (3)$$

$$ZnO\left(e^-_{CB}\right) + O_2 \rightarrow ZnO + O_2^{\bullet -} \quad (4)$$

$$O_2^{\bullet -} + H^+ \rightarrow H_2O^{\bullet} \quad (5)$$

$$H_2O^{\bullet} + H^+ + ZnO\left(e^-_{CB}\right) \rightarrow H_2O_2 + ZnO \quad (6)$$

$$H_2O_2 + ZnO\left(e^-_{CB}\right) \rightarrow OH^{\bullet} + OH^- + ZnO \quad (7)$$

$$MG + OH^{\bullet} \rightarrow CO_2 + H_2O_2 + NO_3^- \quad (8)$$

The resulting $^{\bullet}OH$ produced is a very strong oxidizing agent and can oxidize MG dye into CO_2, H_2O, and mineral acids in LEDs irradiation.

4. Conclusions

This investigation reports the preparation of nanostructured ZnO by a green, cost-effective technique, used effectively in the mineralization of malachite green dye by using LEDs irradiation as a source of visible light. As prepared, ZnO NPs showed better photocatalytic activities for the mineralization of malachite green dye compared to other photocatalysts (TiO_2, BiOCl, $BaCrO_4$, CdS), due to the suitable surface morphology and high efficiency. A significant enhancement of photocatalytic degradation was observed in the system using a combination of Fenton's reagent (Fe^{3+} + H_2O_2) and photocatalyst in the presence of visible light. A remarkable decrease in COD and increase in CO_2 was noticed during the reaction, whereas a tremendous decrease in degradation occurred when pure N_2 purged and increased rapidly on the bubbling of O_2 through the dye suspension. Characterization studies confirmed the external morphology, average particle size, and wurtzite structure of ZnO NPs. This nanostructured-ZnO-assisted photocatalysis promises to be a versatile, inexpensive, eco-friendly, and efficient method for the treatment of textile effluents in general.

Author Contributions: Conceptualization, N.A., J.-W.P., T.A. and V.S.B.; data curation, J.-W.P., B.P., M.M.A. and N.A.; methodology, J.-W.P., B.P., N.B.K. and S.P.; validation, V.S.S., V.S.B. and B.-H.J.; formal analysis, A.G., M.M.A. and N.B.K.; resources, B.-H.J., T.A. and N.B.K.; writing—original draft preparation, V.K.Y., V.S.S., B.P., V.S.B. and N.A.; writing—review and editing, A.G., V.S.S., B.P., V.S.B., V.K.Y., N.B.K., M.M.A., J.-W.P., S.P. and B.-H.J.; supervision, V.K.Y., V.S.S., V.S.B. and B.-H.J.; project administration V.S.S., B.P., V.K.Y., T.A., M.M.A. and B.-H.J.; funding acquisition, N.B.K., M.M.A., T.A. and B.-H.J.; investigation, N.A., V.S.B., V.K.Y., B.-H.J., N.A. and N.B.K.; software, S.P., T.A., B.P., A.G., M.M.A. and N.B.K.; visualization, A.G., S.P. and B.-H.J. All authors have read and agreed to the published version of the manuscript.

Funding: This research received no external funding.

Data Availability Statement: Not applicable.

Acknowledgments: This research work was funded by the Deanship of Research, King Khalid University, Saudi Arabia for large research groups under the grant number R.G. P. 2/59/1443. The authors gratefully acknowledge Taif University Researchers Supporting Project, number (TURSP-2020/242), Taif University, Taif, Saudi Arabia. This work was supported by the Korea Environment Industry and Technology Institute (KEITI) through Subsurface Environment Management (SEM) Projects, funded by the Korea Ministry of Environment (MOE) (No. 2020002480007). VSS & VKY also acknowledges Mody University of Science and Technology, Lakshmangarh and B.P. and V.S.B., acknowledges Govt. Madhav Science PG College, Ujjain, INDIA for providing necessary laboratory facilities.

Conflicts of Interest: The authors declare no conflict of interest.

References

1. Khan, M.M.; Ansari, S.A.; Pradhan, D.; Ansari, M.O.; Han, D.H.; Lee, J.; Cho, M.H. Band gap engineered TiO2 nanoparticles for visible light induced photoelectrochemical and photocatalytic studies. *J. Mater. Chem. A. Mater.* **2014**, *2*, 637–644. [CrossRef]
2. Solanki, V.S.; Ameta, K.L.; Pare, B.; Jonnalagadda, S.B.; Gupta, P. Investigation of photocatalytic mineralisation of Acridine Yellow G dye by BaCrO4 in the presence of eco-friendly LEDs irradiation. *J. Indian Chem. Soc.* **2022**, *99*, 100340. [CrossRef]
3. Javaid, R.; Qazi, U.Y. Catalytic oxidation process for the degradation of synthetic dyes: An overview. *Int. J. Environ. Res. Public Health* **2019**, *16*, 2066. [CrossRef] [PubMed]
4. Rafiq, A.; Ikram, M.; Ali, S.; Niaz, F.; Khan, M.; Khan, Q.; Maqbool, M. Photocatalytic degradation of dyes using semiconductor photocatalysts to clean industrial water pollution. *J. Ind. Eng. Chem.* **2021**, *97*, 111–128. [CrossRef]
5. Jaybhaye, S.; Shinde, N.; Jaybhaye, S.; Narayan, H. Photocatalytic Degradation of Organic Dyes Using Titanium Dioxide (TiO 2) and Mg-TiO 2 Nanoparticles. *J. Nanotechnol. Nanomater.* **2022**, *3*, 67–76.
6. Ameta, K.L.; Sharma, J.; Solanki, V.S. Photocatalytic mineralization of brilliant green dye using bimetallic CeCuO3 nanoparticles in LEDs irradiations: A green and economically viable approach. *Results Chem.* **2022**, *4*, 100438. [CrossRef]

7. Xiao, L.; Zhang, Q.; Chen, P.; Chen, L.; Ding, F.; Tang, J.; Li, Y.; Au, C.; Yin, S. Copper-mediated metal-organic framework as efficient photocatalyst for the partial oxidation of aromatic alcohols under visible-light irradiation: Synergism of plasmonic effect and schottky junction. *Appl. Catal. B: Environ* **2019**, *248*, 380–387. [CrossRef]
8. Li, Y.; Li, M.; Xu, P.; Tang, S.; Liu, C. Efficient photocatalytic degradation of acid orange 7 over N-doped ordered mesoporous titania on carbon fibers under visible-light irradiation based on three synergistic effects. *Appl. Catal. A. Gen.* **2016**, *524*, 163–172. [CrossRef]
9. Xiao, L.; Youji, L.; Feitai, C.; Peng, X.; Ming, L. Facile synthesis of mesoporous titanium dioxide doped by Ag-coated graphene with enhanced visible-light photocatalytic performance for methylene blue degradation. *RSC Adv.* **2017**, *7*, 25314–25324. [CrossRef]
10. Gu, Y.; Guo, B.; Yi, Z.; Wu, X.; Zhang, J.; Yang, H. Morphology modulation of hollow-shell ZnSn(OH)6 for enhanced photodegradation of methylene blue. *Colloids Surf A Physicochem. Eng. Asp.* **2022**, *653*, 129908. [CrossRef]
11. Li, L.; Gao, H.; Liu, G.; Wang, S.; Yi, Z.; Wu, X.; Yang, H. Synthesis of carnation flower-like Bi2O2CO3 photocatalyst and its promising application for photoreduction of Cr(VI). *Adv. Powder Technol.* **2022**, *33*, 103481. [CrossRef]
12. Tomar, R.; Abdala, A.A.; Chaudhary, R.G.; Singh, N.B. Photocatalytic degradation of dyes by nanomaterials. *Mater. Today: Proc.* **2020**, *29*, 967–973. [CrossRef]
13. Govindaraman, L.T.; Arjunan, A.; Baroutaji, A.; Robinson, J.; Ramadan, M.; Olabi, A.G. *Nanomaterials Theory and Applications. Encyclopedia of Smart Materials*; Elsevier: Amsterdam, The Netherlands, 2021; pp. 302–314. [CrossRef]
14. Baig, N.; Kammakakam, I.; Falath, W.; Kammakakam, I. Nanomaterials: A review of synthesis methods, properties, recent progress, and challenges. *Mater. Adv.* **2021**, *2*, 1821–1871. [CrossRef]
15. Zheng, A.L.T.; Abdullah, C.A.C.; Chung, E.L.T.; Andou, Y. Recent progress in visible light-doped ZnO photocatalyst for pollution control. *Int. J. Environ. Sci. Technol.* **2022**. [CrossRef]
16. Yadav, V.K.; Choudhary, N.; Tirth, V.; Kalasariya, H.; Gnanamoorthy, G.; Algahtani, A.; Yadav, K.K.; Soni, S.; Islam, S.; Yadav, S.; et al. A short review on the utilization of incense sticks ash as an emerging and overlooked material for the synthesis of zeolites. *Crystals* **2021**, *11*, 1255. [CrossRef]
17. Khayal, A.; Dawane, V.; Amin, M.A.; Tirth, V.; Yadav, V.K.; Algahtani, A.; Khan, S.H.; Islam, S.; Yadav, K.K.; Jeon, B.-H. Advances in the methods for the synthesis of carbon dots and their emerging applications. *Polymers* **2021**, *13*, 3190. [CrossRef]
18. Rajendran, S.; Inwati, G.K.; Yadav, V.K.; Choudhary, N.; Solanki, M.B.; Abdellattif, M.H.; Yadav, K.K.; Gupta, N.; Islam, S.; Jeon, B.-H. Enriched catalytic activity of TiO2 nanoparticles supported by activated carbon for noxious pollutant elimination. *Nanomaterials* **2021**, *11*, 2808. [CrossRef]
19. Repo, E.; Rengaraj, S.; Pulkka, S.; Castangnoli, E.; Suihkonen, S.; Sopanen, M.; Sillanpää, M. Photocatalytic degradation of dyes by CdS microspheres under near UV and blue LED radiation. *Sep. Purif. Technol.* **2013**, *120*, 206–214. [CrossRef]
20. Gnanamoorthy, G.; Kumar Yadav, V.; Ali, D.; Ramar, K.; Gokhlesh, K.; Narayanan, V. New designing (NH4)2SiP4O13 nanowires and effective photocatalytic degradation of Malachite green and antimicrobial properties. *Chem Phys Lett* **2022**, *803*, 139817. [CrossRef]
21. Dharwadkar, S.; Yu, L.; Achari, G. Photocatalytic degradation of sulfolane using a led-based photocatalytic treatment system. *Catalysts* **2021**, *11*, 624. [CrossRef]
22. Maseera, R.; Sultana, A.; Kiranmai, M. Green Synthesis and Evaluation of Zinc Oxide Nanoparticles from Manilkara Zapota Leaf Extract. *Int. J. Pharma. Sci. Nanotechnol.* **2022**, *15*, 5822–5830. [CrossRef]
23. Demissie, M.G.; Sabir, F.K.; Edossa, G.D.; Gonfa, B.A. Synthesis of Zinc Oxide Nanoparticles Using Leaf Extract of Lippia adoensis (Koseret) and Evaluation of Its Antibacterial Activity. *J. Chem.* **2020**, *2020*, 7459042. [CrossRef]
24. Santhoshkumar, J.; Kumar, S.V.; Rajeshkumar, S. Synthesis of zinc oxide nanoparticles using plant leaf extract against urinary tract infection pathogen. *Resour. Technol.* **2017**, *3*, 459–465. [CrossRef]
25. Karam, S.T.; Abdulrahman, A.F. Green Synthesis and Characterization of ZnO Nanoparticles by Using Thyme Plant Leaf Extract. *Photonics* **2022**, *9*, 594. [CrossRef]
26. Patel, H.; Yadav, K.K.; Choudhary, N.; Kalasariya, H.; Alam, M.M.; Gacem, A.; Amanullah, M.; Ibrahium, H.A.; Park, J.-W.; Park, S.; et al. A Recent and Systemic Approach Towards Microbial Biodegradation of Dyes from Textile Industries. *Water* **2022**, *14*, 3163. [CrossRef]
27. Ajmal, A.; Majeed, I.; Malik, R.N.; Idriss, H.; Nadeem, M.A. Principles and mechanisms of photocatalytic dye degradation on TiO 2 based photocatalysts: A comparative overview. *RSC Adv.* **2014**, *4*, 37003–37026. [CrossRef]
28. Hossain, A.; Abdallah, Y.; Ali, M.A.; Masum, M.M.I.; Li, B.; Sun, G.; Meng, Y.; Wang, Y.; An, Q. Lemon-fruit-based green synthesis of zinc oxide nanoparticles and titanium dioxide nanoparticles against soft rot bacterial pathogen dickeya dadantii. *Biomolecules* **2019**, *9*, 863. [CrossRef]
29. Khan, Z.U.H.; Sadiq, H.M.; Shah, N.S.; Khan, A.U.; Muhammad, N.; Hassan, S.U.; Tahir, K.; Safi, S.Z.; Khan, F.U.; Imran, M.; et al. Greener synthesis of zinc oxide nanoparticles using Trianthema portulacastrum extract and evaluation of its photocatalytic and biological applications. *J. Photochem. Photobiol. B* **2019**, *192*, 147–157. [CrossRef]
30. Rane, N.R.; Tapase, S.; Kanojia, A.; Watharkar, A.; Salama, E.S.; Jang, M.; Jeon, B.H. Molecular insights into plant–microbe interactions for sustainable remediation of contaminated environment. *Bioresour. Technol.* **2022**, *344*, 126246. [CrossRef]
31. Ansari, M.A.; Khan, H.M.; Khan, A.A.; Sultan, A.; Azam, A. Synthesis and characterization of the antibacterial potential of ZnO nanoparticles against extended-spectrum β-lactamases-producing Escherichia coli and Klebsiella pneumoniae isolated from a tertiary care hospital of North India. *Appl. Microbiol. Biotechnol.* **2012**, *94*, 467–477. [CrossRef]

32. Modi, S.; Yadav, V.K.; Choudhary, N.; Alswieleh, A.M.; Sharma, A.K.; Bhardwaj, A.K.; Khan, S.H.; Yadav, K.K.; Cheon, J.-K.; Jeon, B.-H. Onion Peel Waste Mediated-Green Synthesis of Zinc Oxide Nanoparticles and Their Phytotoxicity on Mung Bean and Wheat Plant Growth. *Materials* **2022**, *15*, 2393. [CrossRef] [PubMed]
33. El-Hawwary, S.S.; Abd Almaksoud, H.M.; Saber, F.R.; Elimam, H.; Sayed, A.M.; el Raey, M.A.; Abdelmohsen, U.R. Green-synthesized zinc oxide nanoparticles, anti-Alzheimer potential and the metabolic profiling of: Sabal blackburniana grown in Egypt supported by molecular modelling. *RSC Adv.* **2021**, *11*, 18009–18025. [CrossRef] [PubMed]
34. Degefa, A.; Bekele, B.; Jule, L.T.; Fikadu, B.; Ramaswamy, S.; Dwarampudi, L.P.; Nagaprasad, N.; Ramaswamy, K. Green Synthesis, Characterization of Zinc Oxide Nanoparticles, and Examination of Properties for Dye-Sensitive Solar Cells Using Various Vegetable Extracts. *J. Nanomater.* **2021**, *2021*, 3941923. [CrossRef]
35. Kalasariya, H.S.; Yadav, V.K.; Yadav, K.K.; Tirth, V.; Algahtani, A.; Islam, S.; Gupta, N.; Jeon, B.-H. Seaweed-based molecules and their potential biological activities: An eco-sustainable cosmetics. *Molecules* **2021**, *26*, 5313. [CrossRef] [PubMed]
36. Spoială, A.; Ilie, C.I.; Truscă, R.D.; Oprea, O.C.; Surdu, V.A.; Vasile, B.S.; Ficai, A.; Ficai, D.; Andronescu, E.; Dițu, L.M. Zinc oxide nanoparticles for water purification. *Materials* **2021**, *14*, 4747. [CrossRef] [PubMed]
37. Yadav, V.K.; Yadav, K.K.; Tirth, V.; Gnanamoorthy, G.; Gupta, N.; Algahtani, A.; Islam, S.; Choudhary, N.; Modi, S.; Jeon, B.-H. Extraction of value-added minerals from various agricultural, industrial and domestic wastes. *Materials* **2021**, *14*, 6333. [CrossRef] [PubMed]
38. Yadav, V.K.; Yadav, K.K.; Tirth, V.; Jangid, A.; Gnanamoorthy, G.; Choudhary, N.; Islam, S.; Gupta, N.; Son, C.T.; Jeon, B.-H.; et al. Recent advances in methods for recovery of cenospheres from fly ash and their emerging applications in ceramics, composites, polymers and environmental cleanup. *Crystals* **2021**, *11*, 1067. [CrossRef]
39. Jayaseelan, C.; Rahuman, A.A.; Kirthi, A.V.; Marimuthu, S.; Santhoshkumar, T.; Bagavan, A.; Gaurav, K.; Karthik, L.; Bhaskara Rao, K.V. Novel microbial route to synthesize ZnO nanoparticles using Aeromonas hydrophila and their activity against pathogenic bacteria and fungi. *Spectrochim. Acta Part A Mol. Biomol. Spectrosc.* **2012**, *90*, 78–84. [CrossRef]
40. Fuku, K.; Kanai, H.; Todoroki, M.; Mishima, N.; Akagi, T.; Kamegawa, T.; Ikenaga, N. Heterogeneous Fenton Degradation of Organic Pollutants in Water Enhanced by Combining Iron-type Layered Double Hydroxide and Sulfate. *Chem.-Asian J.* **2021**, *16*, 1887–1892. [CrossRef]
41. Cravotto, G.; di Carlo, S.; Tumiatti, V.; Roggero, C.M.; Bremner, H.D. Degradation of Persistent Organic Pollutants by Fenton's Reagent Facilitated By Microwave or High-intensity Ultrasound. *Environ. Technol.* **2005**, *26*, 721–724. [CrossRef]
42. Modi, S.; Yadav, V.K.; Gacem, A.; Ali, I.H.; Dave, D.; Khan, S.H.; Yadav, K.K.; Rather, S.-u.; Ahn, Y.; Son, C.T.; et al. Recent and Emerging Trends in Remediation of Methylene Blue Dye from Wastewater by Using Zinc Oxide Nanoparticles. *Water* **2022**, *14*, 1749. [CrossRef]
43. Saggioro, E.M.; Körlü, A.E. JCME-EPAKE-AE. Chapter 5—Heterogeneous photocatalysis remediation of wastewater polluted by indigoid dyes. In *Textile Wastewater Treatment*; Oliveira, A.S., Ed.; IntechOpen: Rijeka, Croatia, 2016.
44. Pare, B.; Solanki, V.S.; Gupta, P.; Jonnalgadda, S.B. Visible-light induced photocatalytic mineralization of methylene green dye using BaCrO 4 photocatalyst. *IJCT* **2016**, *23*, 513–519.
45. Maurya, P.K.; Ali, S.A.; Alharbi, R.S.; Yadav, K.K.; Alfaisal, F.M.; Ahmad, A.; Ditthakit, P.; Prasad, S.; Jung, Y.-K.; Jeon, B.-H. Impacts of Land Use Change on Water Quality Index in the Upper Ganges River near Haridwar, Uttarakhand: A GIS-Based Analysis. *Water* **2021**, *13*, 3572. [CrossRef]
46. Al-Namshah, K.S.; Mariappan, S.M.; Shkir, M.; Hamdy, M.S. Photocatalytic degradation mechanism of Ce-loaded ZnO catalysts toward methyl green dye pollutant. *Appl. Phys.* **2021**, *127*, 452. [CrossRef]
47. Tekin, D.; Tekin, T.; Kiziltas, H. Photocatalytic degradation kinetics of Orange G dye over ZnO and Ag/ZnO thin film catalysts. *Sci. Rep.* **2019**, *9*, 17544. [CrossRef]
48. Patil, S.M.; Rane, N.R.; Bankole, P.O.; Krishnaiah, P.; Ahn, Y.; Park, Y.-K.; Yadav, K.K.; Amin, M.A.; Jeon, B.-H. An Assessment of Micro- and Nanoplastics in the Biosphere: A Review of Detection, Monitoring, and Remediation Technology. *Chem. Eng. J.* **2022**, *430*, 132913. [CrossRef]